PHYSICAL REVIEW C VOLUME 58, NUMBER 3 SEPTEMBER 1998

Diversity of fragment sizes in multifragmentation of gold nuclei induced by relativistic ^{3}He ions

J. Brzychczyk,[1,*] E. C. Pollacco,[1,†] C. Volant,[1] D. Lacroix,[2] R. Legrain,[1] K. Kwiatkowski,[3] D. S. Bracken,[3,‡] K. B. Morley,[3,‡] Foxford E. Renshaw,[3,§] V. E. Viola,[3] N. R. Yoder,[3] J. Cugnon,[4] R. G. Korteling,[5] and H. Breuer[6]

[1]*DAPNIA/SPhN CEA/Saclay, F-91191 Gif-sur-Yvette Cedex, France*

[2]*GANIL, BP5027 F-14021 Caen Cedex, France*

[3]*Departments of Chemistry and Physics and Indiana University Cyclotron Facility, Indiana University, Bloomington, Indiana 47405*

[4]*Université de Liège, Institut de Physique, B-4000 Liège 1, Belgium*

[5]*Department of Chemistry, Simon Fraser University, Burnaby, British Columbia, Canada V5A S16*

[6]*Department of Physics, University of Maryland, College Park, Maryland 20742*

(Received 26 February 1998)

The charge-moment technique has been used to study the fragment charge distribution for the ^{3}He(4.8 GeV)+^{197}Au reaction. A large variety of fragment charges characterized by a relative variance $\sim$2.3, is observed for excitation energies around 5.5 MeV/nucleon. Similar signals related to a phase transition are predicted by the percolation model and the statistical multifragmentation model. Effects of detector acceptance and contribution from fission are discussed.
[S0556-2813(98)50309-3]

PACS number(s): 25.70.Pq, 25.55.−e

A nucleus under extreme conditions of temperature can break into many pieces of different sizes. This phenomenon, referred to as multifragmentation, is often related to the possible existence of phase transition in nuclear matter [1–5]. The occurrence of a second-order phase transition (critical behavior) was suggested over ten years ago by the observation of the fragment mass yield exhibiting a power law dependence [6]. Since that time, various statistical tools have been developed in order to extract a signal of critical behavior from the fragment size distributions [7–14]. In particular, Campi in his pioneering work [7] has proposed to study moments of the fragment size distributions. Within the framework of infinite percolation models, the moments of order of 2 or greater diverge at the critical point [7,15]. For finite systems, the divergence is replaced by a maximum near the critical point. This indicates a strong connection with the continuous limit, which makes those quantities of great interest in searching for signals of a critical behavior.

In this contribution, we present the charge moment analysis applied to the ^{3}He(4.8 GeV)+^{197}Au reaction. The transport and thermal properties of this system have been studied in Refs. [16–19]. The interest in this system lies in the fact that the heating process is achieved over a small time scale without leading to sizable compressional or rotational effects. In fact, unlike most heavy-ion induced reactions, the present data show a unique multifragment source [16,18]. In contrast with the present system, extracting signals from heavy-ion reactions can be controversial due to the problem of source separation.

Our first attempt in searching for a critical regime is the examination of the relative variance of the fragment charge distributions. This quantity is expected to reach the largest values in the vicinity of the critical point [7]. As will be shown below, mean values of the relative variance are not distorted by our detector acceptance in case of multifragment events. Experimental evidence of such a signature is scarce [7,20,21]. Two results from emulsion experiments seem to lead to different conclusions [7,20]: one is in accord with a three dimensional percolation model whereas no similar agreement exists in the other. Advantages of the present technique over emulsion experiments are that the preequilibrium contribution can be partially removed from the analysis and that the transferred energies can be evaluated.

The experiment was performed at the Laboratoire National Saturne [16–19]. Both light-charged particles and intermediate-mass fragments ($3 \leqslant Z \leqslant 20$) are fully Z identified with the Indiana Silicon Sphere 4π detector array [22]. In order to minimize contributions from preequilibrium processes, only ''thermal-like'' charged particles are considered in the present analysis. The separation in thermal and fast components has been done via a cutoff in kinetic energies and is based on an analysis of the systematic behavior of the fragment energy spectra [17]. Thermal charged particles are defined to be those with energies below a cutoff energy of $9Z+31$ MeV for $1 \leqslant Z \leqslant 20$, except protons for which a limit of 25 MeV is used.

For a given event j, the charge moment of order k is defined as

$$m_k^{(j)} = \sum_Z Z^k n_Z^{(j)} - (Z_{\max}^{(j)})^k, \tag{1}$$

where $n_Z^{(j)}$ is the number of fragments of charge Z and $Z_{\max}^{(j)}$ is the largest fragment charge in event j. The fragment charge distributions can be characterized by the relative variance, γ_2, given as the following combination of moments

$$\gamma_2^{(j)} = \frac{m_2^{(j)} m_0^{(j)}}{(m_1^{(j)})^2}. \tag{2}$$

*Permanent address: Institute of Physics, Jagiellonian University, 30-059 Kraków, Poland.

†Present address: Laboratoire Pierre Süe, CEA-CNRS, F-91191 Gif-sur-Yvette Cedex, France.

‡Present address: Los Alamos National Laboratory, Los Alamos, NM 87545.

§Present address: Microsoft Corp., Seattle, WA 98195.

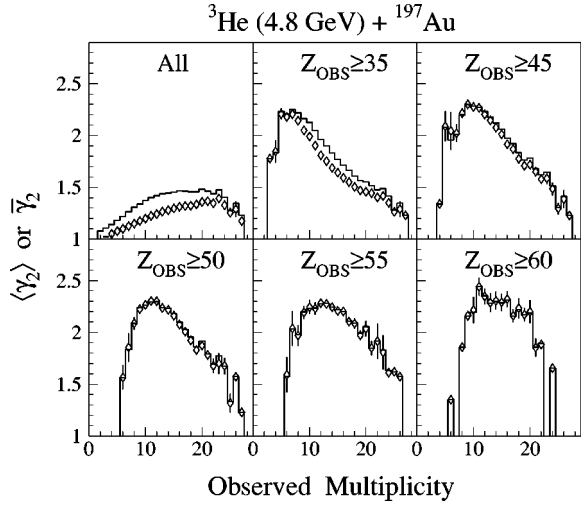

FIG. 1. The experimental average relative variances $\langle\gamma_2\rangle$ (diamonds) and $\overline{\gamma_2}$ (lines) as a function of the observed multiplicity for various conditions on the total observed charge, $Z_{\rm obs}$, (indicated on the figure) for the ^{3}He(4.8 GeV)+^{197}Au reaction.

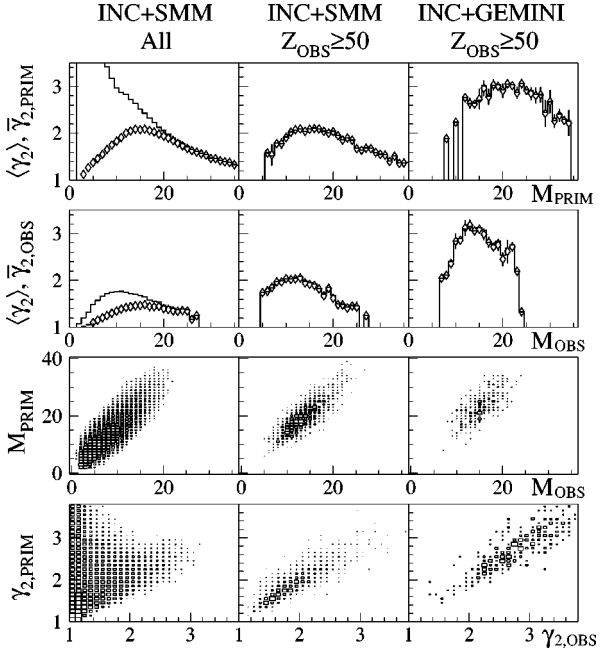

FIG. 2. Correlations between primary and observed quantities obtained by the INC+SMM and INC+GEMINI (weighting option) simulations for the ^{3}He(4.8 GeV)+^{197}Au reaction. Upper frames: $\langle\gamma_2\rangle$ (diamonds) and $\overline{\gamma_2}$ (lines) versus multiplicity before and after filtering. Lower frames: event by event correspondence between primary and observed multiplicities, and between primary and observed relative variances.

This quantity takes the value $\gamma_2=2$ for a pure exponential distribution and $\gamma_2>2$ for a steep power-law distribution [7]. In order to reveal nonstatistical fluctuations, it was proposed to select events according to their multiplicity, M [7,10]. In this work, we examine the two statistical averages

$$\overline{\gamma_2}=\frac{\langle m_2^{(j)}\rangle\langle m_0^{(j)}\rangle}{\langle m_1^{(j)}\rangle^2}, \tag{3}$$

$$\langle\gamma_2\rangle=\langle\gamma_2^{(j)}\rangle. \tag{4}$$

In these expressions, brackets denote the average over events with same multiplicity. The information content of these two quantities is different. The first one corresponds to the width of the average distribution $\langle n_Z\rangle$ for a given multiplicity and has an unambiguous interpretation. The second reflects the average width of individual events and contains also information about fluctuations around the mean distribution. Since these two definitions were previously discussed [7,9,10], we have decided to keep both in our analysis.

Figure 1 displays $\langle\gamma_2\rangle$ (diamonds) and $\overline{\gamma_2}$ (lines) as a function of the observed multiplicity using various threshold values of total detected charge, $Z_{\rm obs}$. Without restriction on $Z_{\rm obs}$, the data contain a large portion of incomplete events and the γ_2 distributions are relatively flat. Increasing the $Z_{\rm obs}$ threshold, the events are progressively more complete and for $Z_{\rm obs}\geqslant50$, 55, and 60, $\langle\gamma_2\rangle$ and $\overline{\gamma_2}$ are equivalent and display a clear maximum at multiplicity $M_{\rm obs}=12\pm1$ with a value of ~2.3.

In order to check that the height and the position of the peak contains a physical meaning and is not a pure artifact of the selection and/or the detector acceptance, we have done simulations with the hybrid INC+SMM and INC+GEMINI models where the coupling is performed event by event. The Liège Intranuclear Cascade Model (INC) [23] describes early stages of the reaction providing input for the statistical multifragmentation model (SMM) [24] or the GEMINI code [25]. After the cascade stage, the heavy remnants (fragmenting systems) are characterized by a broad excitation energy distribution reaching values up to ~10 MeV/nucleon. A stopping time of 35 fm/c was applied to the cascade model in order to reproduce the reconstructed excitation energy distributions [19]. We have used the GEMINI code with the level density parameter $a=A/11$ MeV^{-1} and the SMM with the freeze-out volume $V=3V_0$, where V_0 corresponds to the normal nuclear density. The observables considered in this work are not very sensitive to these parameters.

Figure 2 shows correlations related to the detector acceptance effects. Quantities called ''primary,'' noted $X_{\rm prim}$, are for all charged fragments of the heavy remnant. The term ''observed'' refers to observables ($X_{\rm obs}$) obtained after passing the events through the experimental filter with the same conditions as for the data. The last operation includes cascade protons in order to evaluate their influence on the signal after filtering. The left and central parts of the figure present results of the INC+SMM simulations with no selection (left) and the $Z_{\rm obs}\geqslant50$ selection (center). As another test for the latter selection, the right column in Fig. 2 shows results of the INC+GEMINI event generator. To allow a statistically significant event generation, GEMINI was run with a weighting option which enhances emission of complex fragments. Although this option is not realistic within the context of the model, it is here only used for testing detector effects. The top panel displays $\langle\gamma_2\rangle_{\rm prim}$ and $\overline{\gamma_2}_{,\rm prim}$ versus the primary multiplicity, $M_{\rm prim}$. For all events (top-left), the $\langle\gamma_2\rangle_{\rm prim}$ distribution presents a maximum around 2.1 at $M_{\rm prim}\simeq16$ whereas $\overline{\gamma}_{2,\rm prim}$ exhibits a strong peak (out of the displayed scale) at low multiplicities where evaporation and fission events dominate. Note that a similar behavior is observed in primary INC+GEMINI events (not shown). After applying

the detector filter (next panel below) the observed γ_2 are strongly reduced. Imposing a large $Z_{\rm obs}$ threshold removes evaporation and fission events. For both models, the $Z_{\rm obs} \geqslant 50$ selection reduces $\overline{\gamma_2}$ values in the low multiplicity region down to the same values as $\langle \gamma_2 \rangle$. The maximum of $\overline{\gamma_2}$ is thus sensitive to the selection. On the other hand, the $\langle \gamma_2 \rangle$ appears to be a good observable since the peak is not too strongly affected by the selection.[1] Furthermore, comparing INC+GEMINI to INC+SMM, we observe, as reported in [9], that different models lead to very different positions and heights of the maximum.

In order to better quantify the detector effect on the maxima properties, we also plotted on the bottom part of Fig. 2 the event-by-event correspondence between primary and observed multiplicities and between $\gamma^{(j)}_{2,\rm prim}$ and $\gamma^{(j)}_{2,\rm obs}$. On average, for $Z_{\rm obs} \geqslant 50$, linear correlations between primary and observed quantities occur: $M_{\rm prim} \simeq 1.45 M_{\rm obs}$ and $\gamma_{2,\rm prim} \simeq \gamma_{2,\rm obs}$, independently of the considered model.

Applying these relationships for correcting the experimental distributions, gives a primary multiplicity value of ~ 17 for the maximum of γ_2. The corresponding value of the normalized primary multiplicity $n = M_{\rm prim}/Z_0$, where Z_0 is the total charge of the breaking system, is about 0.25, taking the average charge of the fragmenting system from INC ($\langle Z \rangle \simeq 69$ for $Z_{\rm obs} \geqslant 50$). Thus, the peak characteristics of γ_2 is similar to the one observed in gold data [7,26].

In Fig. 2, we see also clearly the effect of the $Z_{\rm obs}$ selection: large values of $\gamma^{(j)}_{2,\rm prim}$ which correspond to small values of $\gamma^{(j)}_{2,\rm obs}$ are discarded by our selection. Inspecting the detector acceptance shows that these events are mainly fissionlike events correlated to the low multiplicity region. This affects strongly $\overline{\gamma_2}$ but not $\langle \gamma_2 \rangle$. As already pointed out by the authors of Refs. [8,29], fission may influence the γ_2 values. The significant change between primary and observed $\overline{\gamma_2}$ is an illustration of this effect. In order to study the effect of the fission contaminant on γ_2 an additional analysis has been done by removing the two heaviest fragments in the calculations of the moments. In Fig. 3, we report the behavior of both γ_2 when all the fragments but the largest one are considered (left column) and when the two largest fragments are removed (right column). In order to illustrate the effect of the new definition, we show a simulation with INC+GEMINI, without enhanced fragment production, where a large fraction of the events arise from fission processes. In this case, $Z_{\rm obs}$ condition is reduced to $Z_{\rm obs} \geqslant 35$ to allow for appropriate statistics. We first remark that fission gives effectively large values of γ_2 with the original definition. Applying the new definition reduces considerably the γ_2 values. For both INC+SMM and DATA with the selection $Z_{\rm obs} \geqslant 50$, values of $\langle \gamma_2 \rangle$ greater than 2 remain, which indicates that the characteristics of the $\langle \gamma_2 \rangle$ peak is mainly due to multifragmentation events.

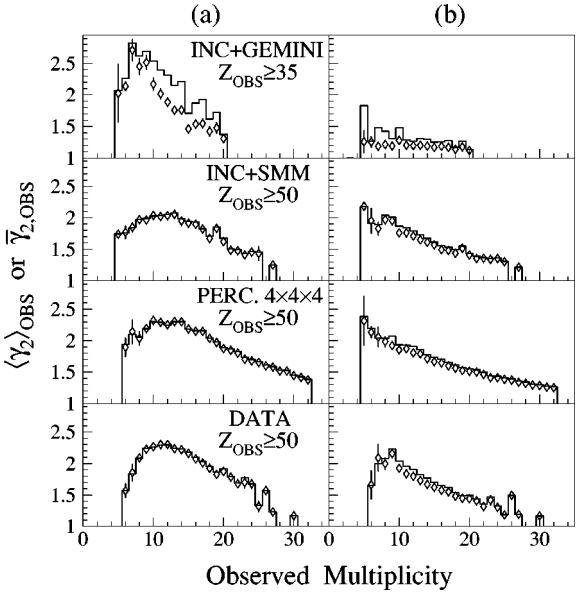

FIG. 3. The observed $\langle \gamma_2 \rangle$ (diamonds) and $\overline{\gamma_2}$ (lines) as a function of the observed multiplicity: (a) calculations without the largest fragment, (b) without the two largest fragments. INC+GEMINI, INC+SMM simulations and data are for the ^{3}He(4.8 GeV)+^{197}Au reaction. Bond-percolation calculations are performed on $4\times4\times4$ cubic lattice. Gating conditions on $Z_{\rm obs}$ are indicated on the figure.

The model simulations show that, in addition to the fact that the data signal could not be understood by a trivial effect, neither the detection acceptance nor the $Z_{\rm obs}$ condition influences $\langle \gamma_2 \rangle$. SMM gives a maximum value of $\langle \gamma_2 \rangle$ of ~ 2.1, at an observed multiplicity close to 12, which is similar to the data signal when excluding the heaviest fragment.

We further investigated another model: a bond-percolation simulation on a $4\times4\times4$ cubic lattice which has a size close to our system. It is known to display a maximum in γ_2 which is connected to critical features present in the infinite case. This model has also been used to check that the limitation on maximum identified charge $Z = 20$ does not preclude the observation of eventual critical events. Making an approximate filtering using effective Z-dependent probabilities of fragment detection extracted from the INC+SMM simulations, shows that a reasonable amount of these events is preserved. The model exhibits before filtering a maximum of $\langle \gamma_2 \rangle \simeq 2$ at a normalized multiplicity $n \simeq 0.28$ (see Ref. [20]). The results after the filtering are shown in Figs. 3(a) and 3(b) for $Z_{\rm obs} \geqslant 50$. The position and height of the peaks are in good agreement with data for all definitions of γ_2. Note that the persistence of γ_2 values greater than 2, further indicates that a large part of critical events survive in the experimental acceptance.

In addition to the relative variance, we have also examined the $\ln(m^{(j)}_3/m^{(j)}_1)$ vs $\ln(m^{(j)}_2/m^{(j)}_1)$ correlation, which can be used in determining the τ critical exponent [7,11]. The plot for experimental events exhibits a linear correlation with the slope parameter $\lambda_{3/2} = 2.2 \pm 0.1$ giving $\tau = 2.17 \pm 0.07$. Similar values were obtained from other experimental data [7,20,27,28]. Nearly the same results are also predicted by the SMM, GEMINI, and percolation models. As was already pointed out [20,29], this slope parameter is only weakly sensitive to the models. On the contrary, the height and the

[1]The authors of Ref. [10] have proposed to use the difference $\delta\gamma_2 = \langle \gamma_2 \rangle - \overline{\gamma_2}$ for studying nonstatistical fluctuations in the fragment size distribution. We see clearly here that $\delta\gamma_2$ may be strongly affected by the presence of fission and evaporation events. Furthermore, given our detector acceptance, the $Z_{\rm obs}$ selection leads to $\delta\gamma_2 \simeq 0$.

position of the maximum of $\langle \gamma_2 \rangle$ are more discriminant.

Since the present results point out signals which could suggest a possible phase transition, it is worthwhile to estimate the corresponding excitation energy. It has been calculated using the total kinetic energy, neutron multiplicity from a mass balance, and appropriate Q value (see for example [19]). The INC+SMM simulations, which reproduce fairly well also the experimental fragment charge distribution, were employed to correct for the detector inefficiency. The excitation energy is correlated with the multiplicity. For events with $Z_{\rm obs} \geqslant 50$, the multiplicity range $M_{\rm obs}=5-25$ corresponds, on average, to the range of excitation energy 4 to 9 MeV/nucleon. The maximum of $\langle \gamma_2 \rangle$ occurs for events with $M_{\rm obs}=12\pm1$ and the average excitation energy of 5.5 ± 0.3 MeV/nucleon.

In conclusion, the relative variance, γ_2, of the charge distribution for thermal-like fragments emitted in the ^{3}He(4.8 GeV)+^{197}Au reaction has been examined. In this reaction, a single heated source is created, avoiding the ambiguity of source recognition [16–18]. Furthermore, in contrast with emulsion experiments, our data allow to reduce the effect of preequilibrium emission. A careful analysis has shown that a maximum of $\langle \gamma_2 \rangle$ is present with a value of ~ 2.3 at a normalized multiplicity $n \simeq 0.25$ (after correction for detector effects). This maximum, which is not due to a trivial effect like detector acceptance, selection or presence of fissionlike events, corresponds to an average excitation energy $E^\star/A \simeq 5.5$ MeV.

The height and the multiplicity position of the γ_2 peak as well as the value of the τ exponent are in agreement with predictions of the three-dimensional percolation model. This confirms the observation of Ref. [7], where a similar system was studied. Although this resemblance between the experimental and percolation signals suggests the presence of a critical behavior in nuclear systems, it is insufficient to conclude on the nature of the transition. The three-dimensional percolation and the liquid-gas universality classes have similar values of the τ critical exponent: 2.18 and 2.21, respectively [27]. The available experimental accuracy does not allow one to discriminate them. Since the τ exponent describes the spectrum of fragment sizes at the critical point (power law), one expects similar critical multiplicities and γ_2 values (locations of the γ_2 maximum) for these two transitions. Thus, the knowledge of another critical exponent is desired.

Such an attempt has been done recently by the EOS Collaboration for the Au(1A GeV)+C system [27,28] studied in reverse kinematics. The authors conclude that the fragment size distributions exhibit a thermodynamic scaling with exponents consistent with the liquid-gas values [28]. The critical point is characterized by the total multiplicity of 22 ± 1 and corresponds to $E^\star/A \sim 5$ MeV. The method used for determining the σ exponent requires events with large multiplicities which are observed at $E^\star/A > 9$ MeV [28,30] and not available in our system. The τ exponent and the excitation energies related to the critical point are similar in the EOS and present results. The critical multiplicity, $M_{\rm prim} \simeq 17$, is obtained here for thermal charged fragments while the EOS value of 22 is for all charged fragments. Further discrepancies may arise also from differences between the systems and the methods used due to finite size effects.

Relative to percolation, the more realistic INC+SMM model also gives a good reproduction of the experimental signal. The analysis of the conditional moments, performed for a Au nucleus within the SMM framework [31], indicates the occurrence of a critical behavior at an excitation energy of about 5 MeV/nucleon and a temperature $T \simeq 6$ MeV. These values fall into a region where a flattening of the caloric curve is observed [31]. A similar correspondence can be deduced from the ALADIN data, where the $\langle \gamma_2 \rangle$ versus $Z_{\rm bound}$ distribution is peaked around $Z_{\rm bound} \simeq 50$ correlated with $E^\star/A \simeq 6$ MeV [21,32]. The coincidence between these two signatures may be accidental or may point to the critical behavior as being due to a reminiscence of the first-order liquid-gas phase transition. Note that Ref. [31] shows indeed, in a particular model at least, that the two signatures are linked.

In summary, overall properties of the relative variance maximum seem to support the possible existence of a phase transition in nuclear systems. However the origin of such a positive signal in finite systems may not be unique [33]. In further analysis, additional studies will be performed involving complementary statistical tools [8,10,12,13], in order to better characterize our observation.

The authors thank A. Botvina and R. J. Charity for the use of their SMM and GEMINI codes and P. Pawłowski for percolation simulations. Financial support of the Commissariat à l'Energie Atomique (France), the U.S. Department of Energy, the National Science Foundation, and the National Council of Canada is acknowledged.

[1] L. G. Moretto and G. J. Wozniak, Annu. Rev. Nucl. Part. Sci. **43**, 379 (1993).

[2] J. P. Bondorf, A. S. Botvina, A. S. Iljinov, I. N. Mishustin, and K. Sneppen, Phys. Rep. **257**, 133 (1995).

[3] W. A. Friedman, Phys. Rev. C **42**, 667 (1990).

[4] D. H. E. Gross, Rep. Prog. Phys. **53**, 605 (1990).

[5] D. Guerreau, Nucl. Phys. **A574**, 111 (1994).

[6] J. E. Finn *et al.*, Phys. Rev. Lett. **49**, 1321 (1982).

[7] X. Campi, J. Phys. A **19**, L917 (1986); Phys. Lett. B **208**, 351 (1988).

[8] M. Ploszajczak and A. Tucholski, Phys. Rev. Lett. **65**, 1539 (1990); Nucl. Phys. **A523**, 651 (1991).

[9] X. Campi and H. Krivine, Z. Phys. A **344**, 81 (1992); Nucl. Phys. **A589**, 505 (1995).

[10] X. Campi and H. Krivine, in *International Workshop on Dynamical Features of Nuclei and Finite Fermi Systems*, Sitges, Spain, 1993 (World Scientific, Singapore), p. 3.

[11] J. B. Elliott, M. L. Gilkes, J. A. Hauger, A. S. Hirsch, E. Hjort, N. T. Porile, R. P. Scharenberg, B. K. Srivastava, M. L. Tincknell, and P. G. Warren, Phys. Rev. C **49**, 3185 (1994); Phys. Rev. C **55**, 1319 (1997).

[12] L. G. Moretto *et al.*, Phys. Rev. Lett. **76**, 372 (1996).

[13] D. Lacroix and R. Peschanski, Nucl. Phys. **A615**, 207 (1997).

[14] A. J. Cole, A. Chabane, M. Charvet, P. Désesquelles, A.

Giorni, D. Heuer, A. Lleres, and J. B. Viano, J. Phys. G **23**, 457 (1997).
[15] D. Stauffer and A. Aharony, *Introduction to Percolation Theory*, 2nd Edition (Taylor & Francis, London, 1992).
[16] K. Kwiatkowski *et al.*, Phys. Rev. Lett. **74**, 3756 (1995).
[17] K. B. Morley *et al.*, Phys. Rev. C **54**, 737 (1996); Phys. Lett. B **355**, 52 (1995).
[18] E. Renshaw Foxford *et al.*, Phys. Rev. C **54**, 749 (1996).
[19] K. Kwiatkowski, A. S. Botvina, D. S. Bracken, E. Renshaw Foxford, W. A. Friedman, R. G. Korteling, K. B. Morley, E. C. Pollacco, V. E. Viola, and C. Volant, Phys. Lett. B **423**, 21 (1998).
[20] B. Jakobsson *et al.*, Nucl. Phys. **A509**, 195 (1990).
[21] P. Kreutz *et al.*, Nucl. Phys. **A556**, 672 (1993).
[22] K. Kwiatkowski *et al.*, Nucl. Instrum. Methods Phys. Res. A **360**, 571 (1995).
[23] J. Cugnon, Nucl. Phys. **A462**, 751 (1987).
[24] A. Botvina, A. S. Iljinov, and I. Mishustin, Nucl. Phys. **A507**, 649 (1990).
[25] R. J. Charity *et al.*, Nucl. Phys. **A483**, 371 (1988).
[26] C. J. Waddington and P. S. Freier, Phys. Rev. C **31**, 888 (1985).
[27] M. L. Gilkes *et al.*, Phys. Rev. Lett. **73**, 1590 (1994).
[28] J. B. Elliott *et al.*, Phys. Lett. B **418**, 34 (1998).
[29] J. Richert and P. Wagner, Nucl. Phys. **A517**, 399 (1990).
[30] J. A. Hauger *et al.*, Phys. Rev. C **57**, 764 (1998).
[31] P. F. Mastinu, M. Belkacem, F. Gramegna, and P. M. Milazzo, Phys. Rev. C **57**, 831 (1998).
[32] J. Pochodzalla *et al.*, Phys. Rev. Lett. **75**, 1040 (1995).
[33] L. Phair, Th. Rubehn, L. G. Moretto, and G. J. Wozniak, Phys. Rev. Lett. **79**, 3538 (1997).